Imaging the equilibrium state and magnetization dynamics of partially built hard disk write heads

R. A. J. Valkass, W. Yu, L. R. Shelford, P. S. Keatley, T. H. J. Loughran, R. J. Hicken, S. A. Cavill, G. van der Laan, S. S. Dhesi, M. A. Bashir, M. A. Gubbins, P. J. Czoschke, and R. Lopusnik

Citation: Applied Physics Letters **106**, 232404 (2015); doi: 10.1063/1.4922374

View online: http://dx.doi.org/10.1063/1.4922374

View Table of Contents: http://scitation.aip.org/content/aip/journal/apl/106/23?ver=pdfcov

Published by the AIP Publishing

Imaging the equilibrium state and magnetization dynamics of partially built hard disk write heads

R. A. J. Valkass,[1,a)] W. Yu,[1] L. R. Shelford,[1] P. S. Keatley,[1] T. H. J. Loughran,[1] R. J. Hicken,[1] S. A. Cavill,[2,3] G. van der Laan,[2] S. S. Dhesi,[2] M. A. Bashir,[4] M. A. Gubbins,[4] P. J. Czoschke,[5] and R. Lopusnik[5]

[1]*School of Physics, University of Exeter, Stocker Road, Exeter EX4 4QL, United Kingdom*
[2]*Diamond Light Source, Harwell Science and Innovation Campus, Didcot OX11 0DE, United Kingdom*
[3]*Department of Physics, University of York, Heslington, York YO10 5DD, United Kingdom*
[4]*Research & Development, Seagate Technology, 1 Disc Drive, Springtown Industrial Estate, Derry BT48 0BF, United Kingdom*
[5]*Recording Heads Operation, Seagate Technology, 7801 Computer Avenue South, Bloomington, Minnesota 55435, USA*

(Received 1 September 2014; accepted 31 May 2015; published online 10 June 2015)

Four different designs of partially built hard disk write heads with a yoke comprising four repeats of NiFe (1 nm)/CoFe (50 nm) were studied by both x-ray photoemission electron microscopy (XPEEM) and time-resolved scanning Kerr microscopy (TRSKM). These techniques were used to investigate the static equilibrium domain configuration and the magnetodynamic response across the entire structure, respectively. Simulations and previous TRSKM studies have made proposals for the equilibrium domain configuration of similar structures, but no direct observation of the equilibrium state of the writers has yet been made. In this study, static XPEEM images of the equilibrium state of writer structures were acquired using x-ray magnetic circular dichroism as the contrast mechanism. These images suggest that the crystalline anisotropy dominates the equilibrium state domain configuration, but competition with shape anisotropy ultimately determines the stability of the equilibrium state. Dynamic TRSKM images were acquired from nominally identical devices. These images suggest that a longer confluence region may hinder flux conduction from the yoke into the pole tip: the shorter confluence region exhibits clear flux beaming along the symmetry axis, whereas the longer confluence region causes flux to conduct along one edge of the writer. The observed variations in dynamic response agree well with the differences in the equilibrium magnetization configuration visible in the XPEEM images, confirming that minor variations in the geometric design of the writer structure can have significant effects on the process of flux beaming. [http://dx.doi.org/10.1063/1.4922374]

Increased hard disk write head fields with consistent rise times on the picosecond timescale are necessary to meet demands for greater storage densities and data rates within perpendicular magnetic recording technology,[1] while avoiding erase after write phenomena[2] and popcorn noise.[3] The writer is a complex three-dimensional nanoscale structure, comprising three distinct regions: the yoke and pole tip connected by a flared confluence region. A number of advanced techniques have been developed to probe the non-uniform magnetic state of the structure, including electron holography,[4] Kerr microscopy,[5–7] and photoemission electron microscopy.[8] Previous experimental studies either have concentrated solely on the pole tip region from the perspective of the air-bearing surface[9,10] or have been unable to provide high enough spatial resolution to resolve the pole tip and confluence region.[11–13] A stable equilibrium state, particularly in the confluence region and pole tip, is essential for producing a reliable write field while the magnetization dynamics within the yoke can significantly alter the amplitude and temporal form of the write field.[14]

In this study, writer structures with a multilayered yoke were imaged with both x-ray photoemission electron microscopy (XPEEM) and time-resolved scanning Kerr microscopy (TRSKM) to provide information about the equilibrium state of the entire writer structure and the dynamic response of the yoke, respectively. Four devices of different geometries were studied to characterize the role of shape anisotropy in the formation and stability of the equilibrium state, as well as any effect of shape on flux conduction.

The sample consisted of a $9 \times 9\text{mm}^2$ wafer piece containing a number of partially built writer structures with the yoke formed from four repeats of a NiFe (1 nm)/CoFe (50 nm) bilayer designed for a high magnetic moment and low coercive field. The geometric parameters, shown in Figure 1(a), were varied to produce writers of different shapes. All writers had a yoke recess (YR) of 1.6 μm, bridge length (BL) of 1 μm, and bridge width (BW) of 0.4 μm. The parameters that varied between writers are shown in Table I. The structures all had uniaxial anisotropy, induced by field annealing, with the easy axis oriented in-plane and perpendicular to the symmetry axis. A total of 12 different writer designs were imaged using XPEEM. The four selected here exhibit the full range of behaviour and demonstrate general principles, while two are directly relevant to recording technology.

The equilibrium domain configuration of the devices was imaged directly by XPEEM using x-ray magnetic

a)Electronic mail: rajv202@ex.ac.uk

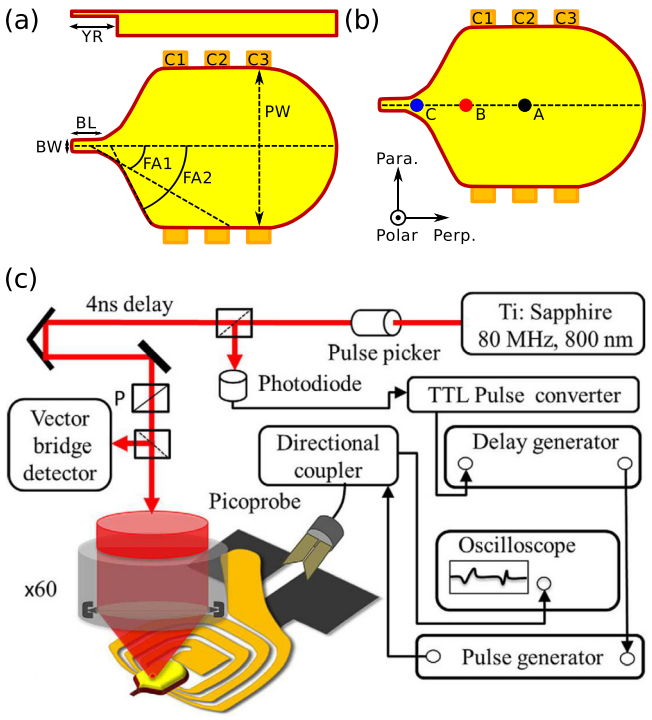

FIG. 1. (a) The geometric parameters varied between different writer structures are shown for a typical paddle-shaped device. C1–C3 are pancake coils embedded beneath the device. The cross section, top, shows the three-dimensional structure of the upper half of the yoke including the yoke recess (YR). (b) The three positions (A, B, and C) at which time-resolved traces were obtained, and the defined coordinate system is shown. (c) The TRSKM setup for measurement of magnetodynamics where P represents a polarizer.

circular dichroism (XMCD) as the contrast mechanism. Images were obtained using left and right circularly polarized soft x-rays at the iron L_3 edge and pre-edge (707 eV and 703 eV, respectively). Images were programmatically corrected for sample drift and between 10 and 40 were averaged together to reduce noise. On-edge images were then normalized relative to their corresponding pre-edge image before the subtraction of opposite polarizations, producing an image showing magnetic contrast. To investigate the stability of the equilibrium magnetic state between write processes, a 2 kG magnetic field was applied *ex situ* along the symmetry axis and then removed before re-imaging.

A schematic layout of the TRSKM setup used for dynamic imaging is shown in Figure 1(c) and has previously been described in detail.[11] The writers were excited with an electrical pulse of 2.2 ns duration (FWHM) and 12.7 V amplitude, shown in Figure 3(a), passed through the coils C1 and C2 at a 1 MHz repetition rate, corresponding to an in-plane field of approximately 200 Oe throughout the yoke. The magnetodynamic response of the writer was probed by an 800 nm laser pulse of 100 fs duration focused onto the writer surface by a 60× microscope objective to give a spot size of ≈600 nm diameter. Each image took approximately 20 min to acquire, with pulses being acquired for 100 ms at each pixel. A 1.5 kG field was applied perpendicular to the symmetry axis of the device to set the equilibrium state before beginning the dynamic measurements. No external bias field or DC was applied during the measurements.

TABLE I. The geometric parameters of each device imaged in this study. The parameters are defined with reference to Figure 1(a).

Parameter	Dev. 1	Dev. 2	Dev. 3	Dev. 4
Paddle Width (PW)(μm)	3.735	20	6.485	6.485
Flare Angle 1 (FA1)(deg)	30	45	30	45
Flare Angle 2 (FA2)(deg)	30	90	62	45

Figure 2(a) shows the equilibrium state of device 1 measured by XPEEM both before and after saturation by a 2 kG field oriented along the symmetry axis. Prior to the application of the field, the magnetization appears to form a large single domain, with orientation orthogonal to the symmetry axis, occupying the yoke and confluence region, with a smaller domain above the back via. After the application of the field, the magnetization has reversed throughout most of the writer. Crystalline anisotropy is clearly dominant since both domains have magnetization perpendicular to the symmetry axis rather than parallel to the symmetry axis as preferred by the shape anisotropy in the device. As the magnetization rotates to align with the applied field, it does so asymptotically through a process of domain rotation. Upon reaching the saturation field, the magnetization irreversibly jumps across the hard axis,[15] relaxing into the antiparallel state.

The sample drift over time, combined with the ≈300nm height of the device above the substrate surface, led to the appearance of high-contrast edge artefacts around some devices. These artefacts have been largely, but not completely, cropped from the images presented here to maximize the available contrast range.

The equilibrium state of device 2, a rectangular reference device, is shown in Figure 2(b). Both before and after the application of the external field, the device exhibits the same flux closure state, with the same magnetization orientation. This was expected, as both the crystalline and shape anisotropy favour the magnetization aligning perpendicular to the symmetry axis of the device.

Devices 3 and 4 (Figures 2(c) and 2(d), respectively) represent more typically shaped devices. Only the flare angles differ between the two devices, giving device 4 a longer, more uniform confluence region than device 3. Devices 3 and 4 both exhibit a qualitatively similar equilibrium state both before and after the application of the external field, with the magnetization within the domains lying largely perpendicular to the symmetry axis. In contrast to device 1, the magnetization does not switch in response to the field applied parallel to the symmetry axis. Here, the smaller shape anisotropy—and therefore higher saturation field—prevents the magnetization from jumping across the hard axis, meaning that the magnetization relaxes back into its original orientation. While the crystalline anisotropy determines the magnetization orientation within an equilibrium domain configuration, the competition between crystalline and shape anisotropy determines the stability of that configuration. The strong shape anisotropy and smaller domains within the pole tip, coupled to this region's complex three-dimensional shape, make a detailed analysis of the behavior of the device within this region difficult.

In order to study the dynamic behaviour of different device designs, nominally identical copies of devices 3 and 4

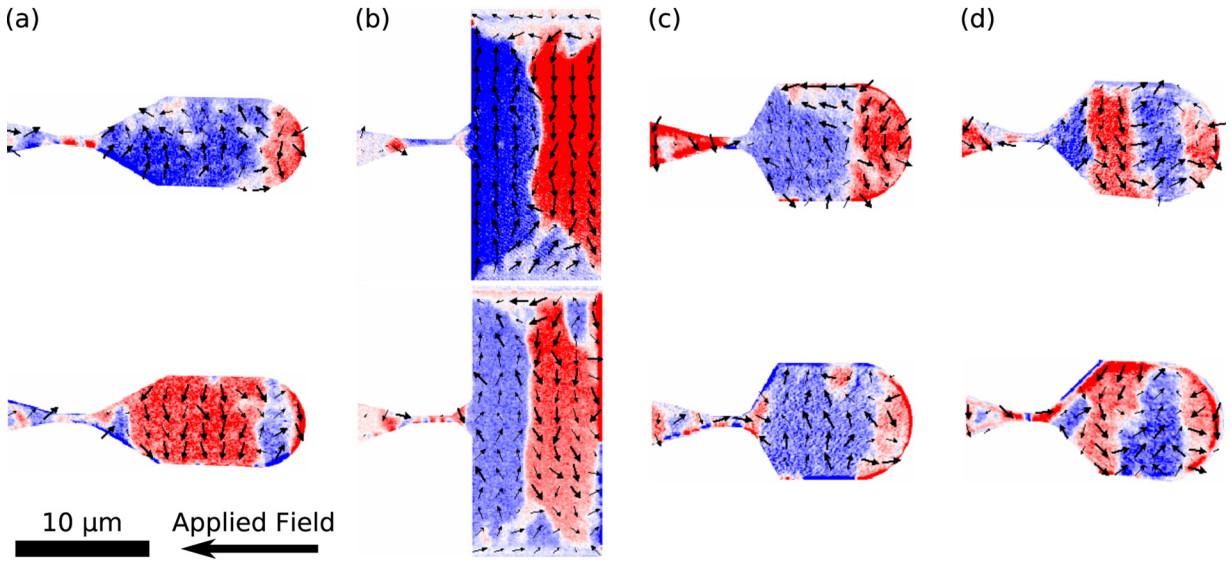

FIG. 2. XPEEM images of the magnetic domain structure of devices 1–4 (panels (a)–(d)) both before (top) and after (bottom) the application and removal of a 2 kG magnetic field parallel to the symmetry axis of the devices. The color represents the component of magnetization perpendicular to the symmetry axis. All images are shown on the same color scale. The direction and length of the arrows represent the in-plane orientation and magnitude of **M**, respectively. The variation of |**M**| across each device is likely due to inhomogeneity on a scale beyond the spatial resolution of the XPEEM, or out of plane components of **M**.

were also studied by TRSKM. The results are compared to XPEEM images obtained before the application of the field parallel to the symmetry axis, as this latter field was intended to test the stability of, rather than reset, the equilibrium state. While minor variations in the equilibrium state are expected between nominally identical devices, these variations do not change the character of the observed dynamic response. Figures 3(d) and 3(e) show the dynamic response of devices 3 and 4, respectively. The pulsed current is flowing upwards in all frames, resulting in an in-plane magnetic field pointing to the right.

For device 3, the perpendicular channel shows a strong signal along the symmetry axis, and also in the middle of the upper half of the yoke from 1.94 ns onwards. The equilibrium state suggested by the TRSKM imagery for device 3 is shown in Figure 3(b) and is in qualitative agreement with the XPEEM results presented here. However, the perpendicular channel also shows weak contrast at 0.3 ns delay, before the arrival of the driving pulse, suggesting poor relaxation behaviour for this design under these driving conditions.

TRSKM images of device 4 show flux conducted along the bottom edge of the device in the perpendicular channel. With the driving field oriented towards the back of the device, this suggests that the magnetization within the bottom half of the confluence region is canted towards the back of the device, whereas the magnetization within the upper half of the confluence region is canted towards the pole tip. Flux conduction along the top edge of the device would lead to the formation of a tail-to-tail domain wall in the upper half of the yoke, whereas a head-to-tail wall would be formed in

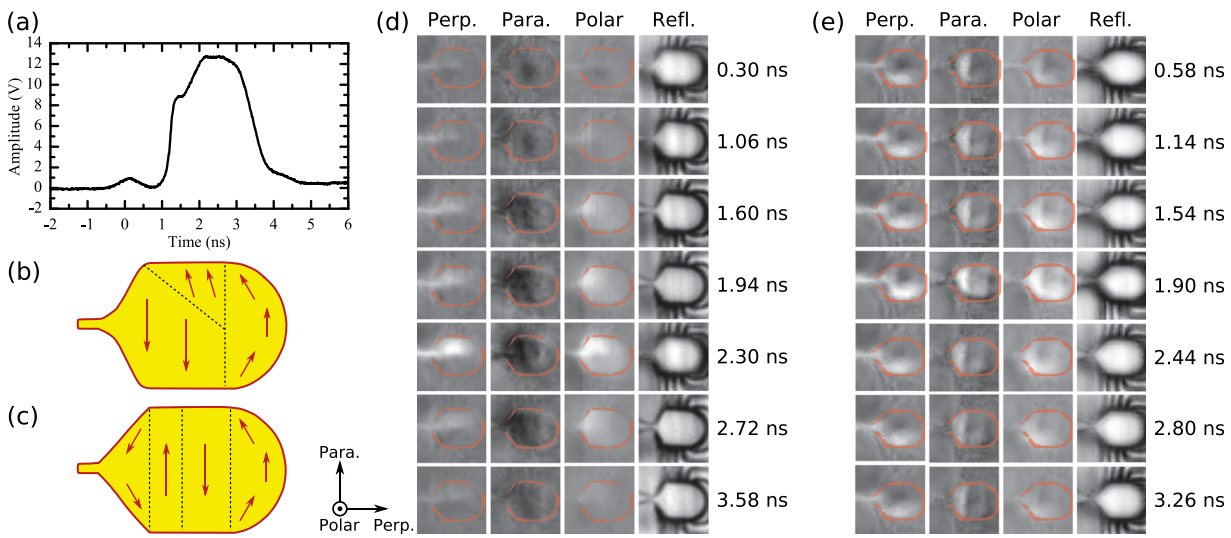

FIG. 3. (a) The driving pulse used to excite the writers during TRSKM measurements. (b) Equilibrium state of device 3 derived from TRSKM. (c) Equilibrium state of device 4 derived from TRSKM. (d) Time-resolved imagery of device 3. (e) Time-resolved imagery of device 4. Black and white correspond to changes in the magnetization in the −/+ *x*-direction, +/− *y*-direction, and −/+ *z*-direction for the perpendicular, parallel, and polar components, respectively. The red outline, derived from the reflectivity image of the device, has been overlaid to guide the eye.

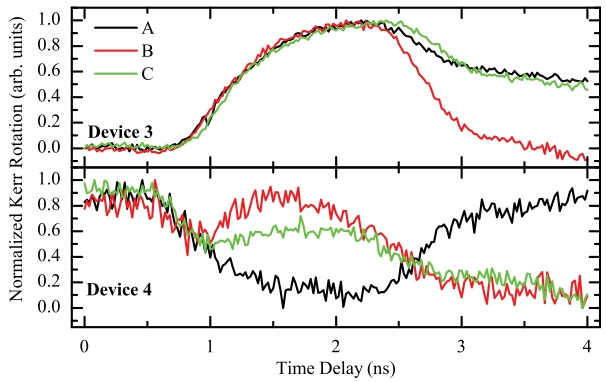

FIG. 4. Perpendicular component of the time resolved signal acquired at three positions (shown in Figure 1(b)) in the yokes of device 3 (top) and device 4 (bottom). Traces have been normalized for each position.

the lower half of the yoke. As the latter costs less dipolar energy, flux conduction along the lower edge of the device is energetically favourable. While the XPEEM images show that this design has a striped equilibrium domain structure, which should result in flux beaming along the symmetry axis of the yoke,[16] the shape anisotropy of the longer confluence region appears to be disrupting flux conduction.

Figure 4 shows the time resolved Kerr rotation observed at different positions on devices 3 and 4 (defined in Figure 1(b)). In device 3, the magnetization initially rotates in unison at each of the three measured points. However, the magnetization at position B relaxes quicker than at positions A and C. This suggests that the yoke drives flux conduction along the length of the device. In device 4, the magnetization exhibits more complex behavior. This is due to the flux beam in this device being positioned towards the lower edge, rather than along the symmetry axis. The dynamics of device 4 are therefore less well defined and depend on the detailed ground state of the device. Positioning of the focused laser spot on a domain wall may also complicate the signal further. However, it is possible to see that positions B and C, while initially rising with position A, then lag behind position A by ≈2ns, as can also be seen in Figure 3(e). This indicates the presence of residual flux propagating through the writer after the driving pulse has ceased, potentially leading to erase-after-write errors in devices of this shape.[17]

XPEEM has been used to image the equilibrium state of partially built hard disk write heads, showing detail in the confluence region and pole tip. These images suggest that the crystalline anisotropy dominates the equilibrium state configuration. The competition between crystalline and shape anisotropy determines the stability and repeatability of the equilibrium state. The equilibrium state domain structures suggested by the XPEEM images are in agreement with the images obtained by TRSKM. TRSKM images of the magnetodynamics in differently shaped writers further suggest that a longer, more acute confluence region may negatively impact flux conduction into the pole tip. By combining the results of both XPEEM and TRSKM, it is possible to better understand both the equilibrium state domain configuration and the dynamics within the yoke. Furthermore, the general principles presented here regarding the influence of geometric parameters on high frequency magnetization dynamics can elucidate the mechanisms of magnetic flux conduction within other micro- and nano-scale patterned materials. In order to further understand the writer dynamics, particularly within the nanoscale pole piece, a time-resolved XPEEM study is required.

The authors thank Diamond Light Source for access to beamline I06 (SI9287-1) that contributed to the results presented here.

The authors gratefully acknowledge financial support from the Seagate Plan.

[1]R. E. Fontana, S. R. Hetzler, and G. Decad, IEEE Trans. Magn. **48**, 1692 (2012).
[2]O. Heinonen, A. Nazarov, and M. L. Plumer, J. Appl. Phys. **99**, 08S302 (2006).
[3]F. H. Liu and M. H. Kryder, J. Appl. Phys. **75**, 6391 (1994).
[4]J. J. Kim, K. Hirata, Y. Ishida, D. Shindo, M. Takahashi, and A. Tonomura, Appl. Phys. Lett. **92**, 162501 (2008).
[5]M. R. Freeman and J. F. Smyth, J. Appl. Phys. **79**, 5898 (1996).
[6]M. R. Freeman, A. Y. Elezzabi, and J. A. H. Stotz, J. Appl. Phys. **81**, 4516 (1997).
[7]M. R. Freeman, G. M. Steeves, G. E. Ballentine, and A. Krichevsky, J. Appl. Phys. **91**, 7326 (2002).
[8]K. Fukumoto, W. Kuch, J. Vogel, F. Romanens, S. Pizzini, J. Camarero, M. Bonfim, and J. Kirschner, Phys. Rev. Lett. **96**, 097204 (2006).
[9]A. Taratorin and K. Klaassen, IEEE Trans. Magn. **42**, 157 (2006).
[10]P. Czoschke, S. Kaka, N. J. Gokemeijer, and S. Franzen, Appl. Phys. Lett. **97**, 242504 (2010).
[11]P. Gangmei, P. S. Keatley, W. Yu, R. J. Hicken, M. A. Gubbins, P. J. Czoschke, and R. Lopusnik, Appl. Phys. Lett. **99**, 232503 (2011).
[12]W. Yu, P. Gangmei, P. S. Keatley, R. J. Hicken, M. A. Gubbins, P. J. Czoschke, and R. Lopusnik, Appl. Phys. Lett. **102**, 162407 (2013).
[13]W. Yu, P. S. Keatley, R. J. Hicken, M. A. Gubbins, P. J. Czoschke, and R. Lopusnik, IEEE Trans. Magn. **49**, 3741 (2013).
[14]Z. Guo and E. Della Torre, IEEE Trans. Magn. **32**, 1136 (1996).
[15]C. Daboo, J. A. C. Bland, R. J. Hicken, A. J. R. Ives, and M. J. Baird, Phys. Rev. B: Condens. Matter Mater. Phys. **47**, 11852 (1993).
[16]M. L. Mallary, J. Appl. Phys. **57**, 3952 (1985).
[17]D. Z. Bai, J.-G. Zhu, P. Luo, K. Stoev, and F. Liu, IEEE Trans. Magn. **42**, 473 (2006).